Available online at www.sciencedirect.com

ScienceDirect

Procedia CIRP 88 (2020) 527–532

www.elsevier.com/locate/procedia

13th CIRP Conference on Intelligent Computation in Manufacturing Engineering, CIRP ICME '19

Image-based system and artificial neural network to automate a quality control system for cherries pitting process

Gabriele Baiocco[a,*], Daniele Almonti[b], Stefano Guarino[c], Flaviana Tagliaferri[c], Vincenzo Tagliaferri[b], Nadia Ucciardello[b]

[a] University of L'Aquila, Dipartimento di Ingegneria Industriale e dell'Informazione e di Economia , Via G. Gronchi, 18, 67100 L'Aquila, Italy
[b]University of Rome 'Tor Vergata', Department of Enterprise Engineering, Via del Politecnico, 1, 00133, Rome, Italy
[c]University of Rome 'Niccolò Cusano', Department of Engineering, Via Don Carlo Gnocchi, 3, 00166, Rome, Italy

* Corresponding author. Tel.: +39-0672597591; *E-mail address:* gabriele.baiocco@uniroma2.it

Abstract

This work proposes a non-destructive quality control for a pitting process of cherries. A system composed of a video camera and a light source records pictures of backlit cherries. The images processing in MATLAB environment provides the dynamic histograms of the pictures, which are analysed to state the presence of the pit.
A feedforward artificial neural network was implemented and trained with the histograms obtained. The network developed allows a fast detection of stone fractions not visible by human inspection and the reduction of the accidental reject of properly manufactured products.

Peer review under the responsibility of the scientific committee of the 13th CIRP Conference on Intelligent Computation in Manufacturing Engineering, 17-19 July 2019, Gulf of Naples, Italy.

Keywords: neural networks; process automation; quality control; image analysis; computer vision

1. Introduction

In the last decade, fruits and vegetables have been increasingly consumed due to their health-promoting constituent [1]. These products easily perish and, being intended for human consumption, industries look for effective quality assessment methods both for food freshness and manufacturing process. Nowadays, several non-destructive methodologies for the inspection, classification and quality control of different products have been developed and applied [2-5]. Among these techniques for quality and safety assessment, imaging methodologies have been extensively applied [6; 7].

Anyway, in an industrial contest characterized by a growing competitiveness, efficiency and rapidity have become crucial for the management of manufacturing systems. Despite the human component is still a focal point for every manufacturing process, the support of artificial intelligence and big data analysis may represent a remarkable enhancement for the industrial systems. In this context, and specifically in multivariable systems analysis', Artificial Intelligence and particularly the artificial neural networks (ANN) find a prominent position [8]. Their principal feature is the ability to learn from an experimental dataset and provide a model capable to give accurate responses when interrogated with unknown data. The application fields are several and include the aid of decision-making processes, classification tasks, phenomena prediction, design optimization and materials characterization [9-20]. Images recognition is one of the most exploited applications within artificial intelligence tasks. Several methods have already been employed such as fuzzy reasoning [21], linear classifier [22], texture analysis [23], expert systems [24] and neuro-fuzzy inference [25]. Since the texture is the main visual content, several kinds of texture representations have been used in previous studies, such as the Local Binary Pattern [26] and the Webber Local Descriptor [27]. The aforementioned works use support vector machines; anyway, the convolutional neural network [28] represents the methodology used to reach the state of

Peer review under the responsibility of the scientific committee of the 13th CIRP Conference on Intelligent Computation in Manufacturing Engineering, 17-19 July 2019, Gulf of Naples, Italy.
10.1016/j.procir.2020.05.091

art in several pattern recognition problems [29; 30]. In [31] is presented a paper where an artificial neural network was exploited in order to ease the welding defects detection by means of radiographic images analysis. In that paper, an ANN was trained with the geometric features of defects. Therefore, the algorithm provides for different steps such as the location of the region of interest, the discontinuities detection and the features' extraction. The extrapolation of the critical information among the entire input variables is a typical problem of these approaches. The work presented by Costa et al. [32] is an example of the topic introduced. They extrapolate the information from the spectrogram related to audio signals in a music identification problem. The study involves the extraction of critical information by means of the visual content of the audio signal, simplifying the problem from signal analysis to pattern recognition.

In industrial productions of food, automated images recognition systems were applied for classification problems [33-35] and quality inspection tasks [36-38] by means of computer-integrated vision [39-43]. Anyway, the aforementioned papers concern the investigation of superficial features and any works concerning the investigation of the internal characteristics of food have been presented. In the present paper, the automation of a quality control process for a cherries stoning system based on a not destructive investigation of the internal feature is proposed. The aim of the work was the detection of pit fractions within the pulp of a cherry. Since pulp and stone feature different absorption coefficients, a brilliance analysis of backlit cherries was chosen as the method for discerning the eventual presence of pit or pit fragment inside the pulp. The core of the system created is the histogram analysis of backlit cherries pictures, exploited to train an artificial neural network able to state the stone presence. The network implemented allows the detection of the pit or its fractions inside the cherries pulp in an automated manner, giving a fast response with an enhanced resolution with respect to the visual inspection.

2. Materials and Methods

The typologies of cherries exploited in the experimental tests are resumed in Table 1. Particularly, two different qualities of cherries and five different sizes were considered. A classification was necessary as the stone dimension does not grow linearly with the diameter of the cherry. Furthermore, different qualities of cherries feature a different percentage of pulp. Therefore, the same stone fragments produce different histograms in function of the cherries diameter and quality.

Table 1 Cherries classification

Diameter (mm)	Cherries typology	
	A	B
14-16	x	-
16-18	x	-
20-22	x	x
22-24	x	x
24-26	x	-

In order to acquire images of backlit cherries, the experimental set up represented in Figure 1 was arranged.

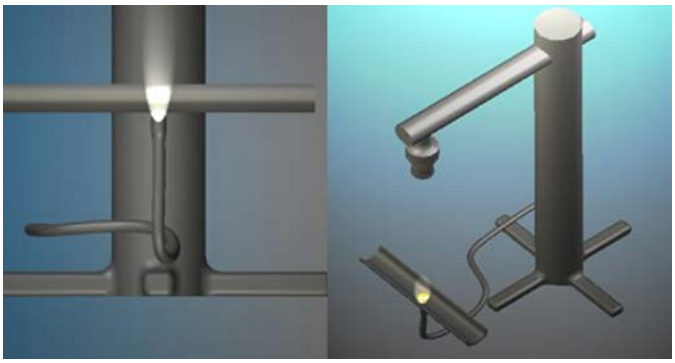

Fig. 1 scheme of the experimental setup.

A support for the cherries was placed between a light source and a video camera. The optical instrumentation used during the experimental activities was a digital video camera PIXERA Mod 150ES, which captures pictures in the RGB format. The camera was equipped with a light unit Nikon with a lens model AF NIKKOR 28-55 mm. The illumination system was composed of an optical fiber powered by a current transformer. Because of the light beam deviation, the source was placed as close as possible to the cherries support in order to focus the light beam on the cherry.

The wavelength of the light source was defined in consequence of a spectrographic analysis of the cherries. This analysis, reported in Figure 2, showed how the best transmittance is given by wavelengths of 1300 nm and 1650 nm. A source characterized by 1300 nm was chosen for the experimental tests.

The defects of a not correct pitting operation were represented by the residues of the stone inside the pulp. Particularly, an entire, a half, a quarter and an eighth of the cherries stone was considered.

Since during the manufacturing process the cherries roll on tubular support, their position under the camera is random. The same occurs for the stone fragments embedded in the pulp. Therefore, the histograms extrapolated from pictures representing the same cherry with the same pit fraction could be different. For each stone fragments, the cherries were recorded in six different positions. A total of 2520 pictures were acquired, equally divided for quality, size and stone fraction.

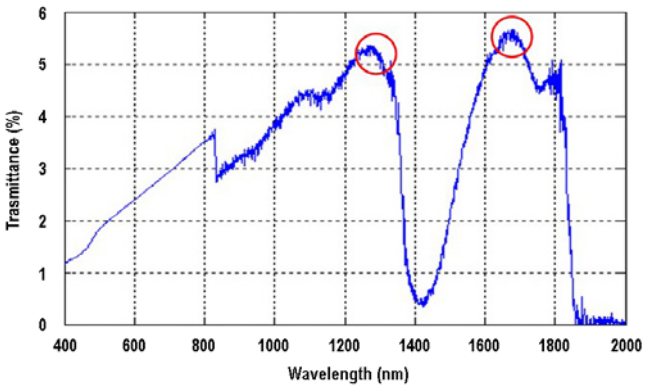

Fig. 2. spectrographic analysis results with transmittance percentage function of wave lengths.

2.1 Assessment of spectral analysis and images processing

During the pictures acquisition, it was evident the low information given by the blue channel while the red channel was saturated, as shown in Figure 3. In addition, the histograms achieved from the combination of green and red channel led to a misclassification of the cherries. Indeed, the histograms obtained from cherries with an eighth of stone and properly pitted are similar, as highlighted in Figure 4. Therefore, only the green channel was considered for the neural network training.

The images concerning the green channel were elaborated in MATLAB environment for the extrapolation of the histograms. Being the resolution of the camera 1392×1040 and the images acquired in a single channel, MATLAB creates a matrix which dimensions was 1392×1040, 1447680 elements. Each element assumed a value ranged between 0 and 255, corresponding to the pixel colour intensity in a grey-scale. Following, a matrix 256×2 was created; the first column refers to the different level of the colour intensity and the second to the number of pixels characterized by a given level. A further row was then added in order to consider the other variable of the network, the cherries diameter, obtaining a vector 257×2. The quality of the cherry investigated was not included in the variable set since from a preliminary analysis resulted that it does not affect the histograms shape.

2.2 Neural network implementation

The dynamic histogram analysis was performed by means of an artificial neural network. To that purpose, an ANN composed of a single hidden layer was implemented with a 257 neurons in the input layer, 8 in the hidden layer and 1 in the output layer. The ANN structure is represented in Figure 5. The transfer function exploited for both the layers' connection was the log-sigmoidal transfer function.

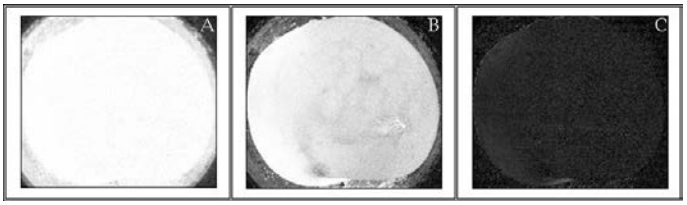

Fig. 3 images of the RGB format in the scale of grey for the A) red B) green c) blue channel.

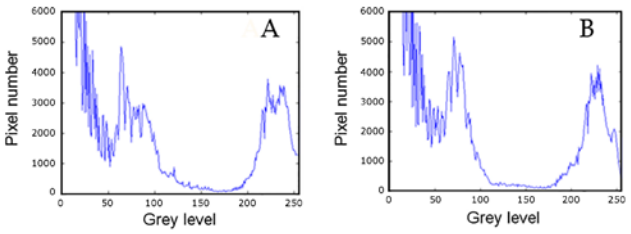

Fig. 4 histogram corresponding to a) pitted cherry b) cherry with an eighth of stone.

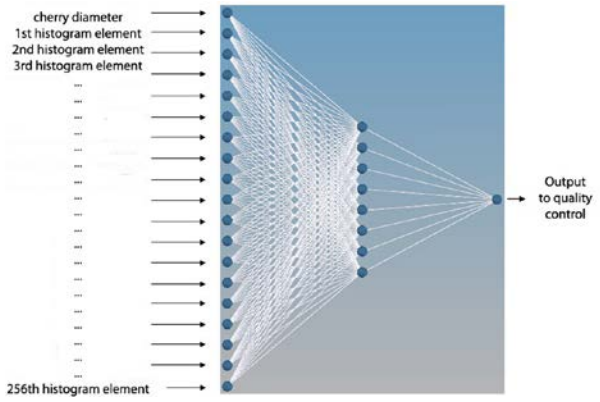

Fig. 5 Artificial neural network scheme

For the neural network training, 1761 histograms of 2520 acquired were used for the training while the 759 left were applied for the validation phase. For each histogram used in the training matrix, a discrete output variable was associated. While the value "0" corresponds to a cherry with a stone of a stone fraction, "1" is associated with cherries properly processed during the pitting operation. The training algorithm was the resilient backpropagation algorithm with a learning rate of 0.01. Finally, the stop parameter was defined; particularly, a maximum number of epochs equal to 2000 and with an error equal to 1e-5 were set. The performance function chosen was the Mean Squared Normalized.

3. Results

Some of the 2520 picture acquired are reported in Figure 6, with the corresponding histogram. Particularly, the images reported refer to the quality "A" with the diameter of the cherries ranged between 14 and 16 mm with a) entire pit, b) a half of the pit, c) a quarter of the pit, d) an eighth of the pit, e) any pit. Furthermore, in order to resume the data acquired from 2520 pictures all the histograms, obtained from the same kind of cherries in terms of quality and size, were superimposed to obtain a single graph. In Figure 7 the results obtained for the cherries with diameters ranged in 14-16 [mm] are reported; the histograms belong to cherries of A.

The histograms analysis showed a clear correlation with the pit fraction. When an entire pit was embedded within the pulp, the great part of the pixels was characterized by dark tones of grey due to the low quantity of light passing through the cherry. This implies the presence of a single peak in the histogram at the darker tones of grey. When smaller stone fractions were considered, the light and middle tones of grey increased due to a reduced stone portion affecting the light transfer. Therefore, a second peak could be identified at the lightest tones of grey. The smaller is the stone portion the greater is the peak shift towards the light tones of grey. A small dispersion due to the variability of the meat of the cherries characterizes the peak. The results obtained for the other categories are not reported but the previous consideration can be generalized for the whole pictures acquired.

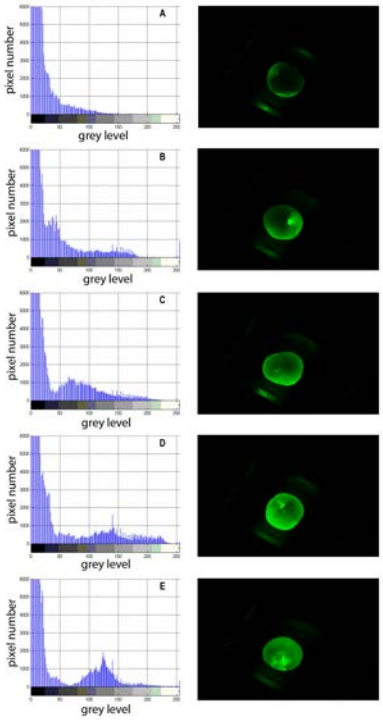

Fig. 6 pictures and histograms of a cherry with a) entire stone, b) a half, c) a quarter, d) an half, e) an eighth of the tone.

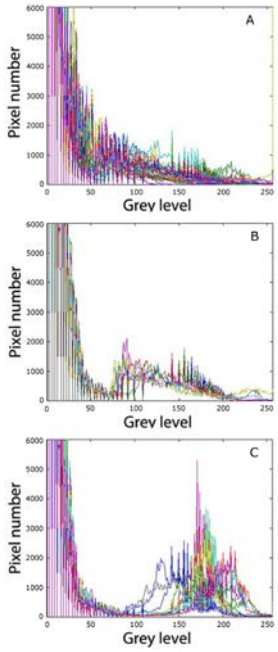

Fig. 7 superimpositions of the histograms of quality A cherries A) with the entire pit B) with an eighth of the pit C) without pit

Also, considering the same stone fraction, a slight shifting of the peak towards the light tone of grey was visible with the growth of the cherry diameter. This behaviour was attributed to the non-proportioned growth of pulp and stone entailed by the cherry dimension. As the ratio between pulp and stone growth with the diameter, the count of the light pixel increase and the peaks feature a larger base. In Figure 8, the histograms of A quality cherries with an eighth of the pit within the pulp are reported for diameters of A) 14-16 mm B) 16-18 mm C) 20-22 mm D) 22-24 mm E) 24-26 mm.

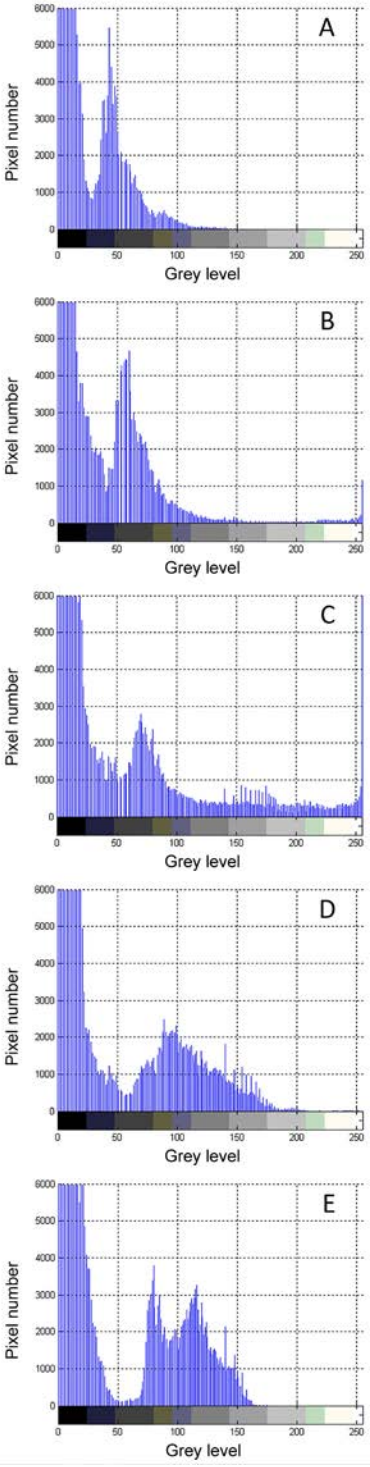

Fig. 8 histograms of cherries with an eighth of the pit for different size.

The analysis of the network results concerned the performance of the validation by comparing the difference between the actual and the simulated output. On a validation set of 759 images, the pictures wrongly interpreted are 59, for an accuracy of 92.3 %. The results are reported in Table 2.

Table 2 error committed in the validation phase

Cherry diameter (mm)	Stone fragment					Misclassified images
	0	*1/8*	*1/4*	*1/2*	*1*	
14-16	0	0	0	0	0	0
16-18	4	0	0	0	0	4
20-22	17	1	0	0	0	18
22-24	13	0	0	0	0	13
24-26	20	4	0	0	0	24
Misclassified images	54	5	0	0	0	

The 91,5% of the misclassified cherries images, concern cherries without pit. The network has learnt and could actually recognize all the histograms of not properly pitted cherries while its weight assignment disadvantages the detection of properly manufactured cherries. Since the training was developed with an 80% of histograms from cherries with a pit fraction within the pulp, this behaviour was expected. Furtherly, dark spots on the cherries surface were detected and confused with stone portions. The other kind of error committed by the network is related to the incorrect identification of an eighth of the pit. The random placement of the cherries, because of the small dimension of the pit portion, may be such that the stone fragment is aligned with the camera. This reduces the dark pixel content of the histogram. Moreover, there is a strong similarity with the histograms of cherry without the stone, as shown in Figure 9, and it is stronger the bigger is the cherries dimension.

Furthermore, it was evident how the error number increased with the cherries diameter. This behavior was justified considering the histograms shape modification in function of this parameter. The shift of the second peak towards the lighter tones of grey was associated both with the reduction of the stones dimension and with the cherries diameter increment. Therefore, when large not stoned cherries were analyzed, histograms with an increased shift of the second peak to the lighter tones of grey were detected. This behaviour was wrongly interpreted by the network causing the increase of the error rate, even more if pitted cherries or small stone fractions were analyzed as they feature a histograms peak heavily shifted towards the light tones of grey. In the test phase, 252 cherries were furtherly investigated. The focus laid on cherries correctly pitted and characterized by an eighth of the pit. The results obtained in the generalization step are reported in Table 3. The network response is characterized by an error of 4.8% considering the cherries without pit not properly classified and 6.3% for the cherries with an eighth of the pit. Therefore, the network features an accuracy of 88.9%, close to the result obtained in the validation step. Furtherly, considering the goal of the stoning quality assessment as the identification of not properly pitted cherries the performance of the system grows to 93.7%. However, the results obtained with this method can be furtherly improved. Being the instrumentation inexpensive it is possible to implement several control stations on the same production line.

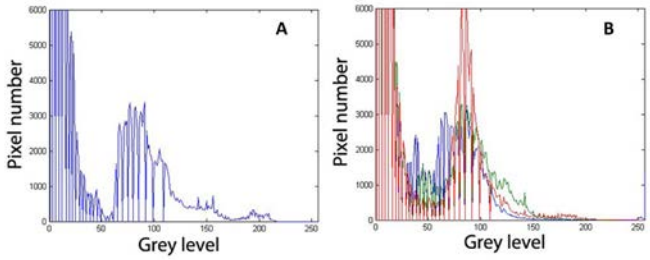

Fig. 9 histograms of cherries without stone (A) and superimposition of the histogram A with the histogram for an eighth of pit (B).

Table 3 error committed in the generalization phase

Cherry diameter (mm)	Stone fragment		Misclassified images
	0	*1/8*	
14-16	0	3	3
16-18	2	6	8
20-22	2	4	6
22-24	2	3	5
24-26	6	0	6
Misclassified images	12	16	

Two and three control stations placed in series would results in a reduction of the error rate of about, respectively, one and two orders of magnitude. In addition, it is possible to set two cameras oriented in orthogonal axis to reduce the error caused by the random placement of the cherry during the analysis.

4. Conclusion

In the paper proposed, an automated system for the quality control of a pitting system for cherries production was developed. In MATLAB environment, a code capable to extrapolate essential information in a simple and brief manner from the pixel content of backlit cherries picture was implemented. The histograms analysis allowed to correlate several shape with the eventual presence of pit fraction embedded in the pulp.

Following, a neural network was implemented and trained with the histograms acquired. The validation analysis showed an increasing error rate with cherry diameter increment. Particularly, the misclassification regarded pitted cherries and the smallest pit fraction investigated, an eight of pit. This was due to the fact that cherries diameter increment and pit fraction decrement produced the same effect on the histogram shape. Anyway, during the network testing an accuracy of 93.7% was reached that can be furtherly increased due to the simplicity of the system implemented. Furthermore, the software implemented can be connected with a sorting system of the cherries, activated in function of the network output.

The method implemented allows the detection of pit fraction up to an eight, in contraposition with the visual inspection performed that lead to the detection of pit fraction up to a quarter. Moreover, the system allows a faster detection of pit fraction not visible by human. On the light of the performance achieved, the methodology proposed for the quality control of a cherries pitting system can be considered valuable.

References

[1] Padayachee A, Day L, Howell K, Gidley MJ. Complexity and health functionality of plant cell wall fibers from fruits and vegetables. Crit Rev Food Sci Nutr 2017;57:59–81. doi:10.1080/10408398.2013.850652.

[2] Elvira L, Sampedro L, Montero de Espinosa F, Matesanz J, Gómez-Ullate Y, Resa P, et al. Eight-channel ultrasonic device for non-invasive quality evaluation in packed milk. Ultrasonics 2006;45:92–9. doi:10.1016/j.ultras.2006.07.011.

[3] Grombe R, Kirsten L, Mehner M, Linsinger TPJ, Emons H, Koch E. Feasibility of non-invasive detection of engineered nanoparticles in food mimicking matrices by Optical Coherence Tomography. Food Chem 2014;153:444–9. doi:10.1016/J.FOODCHEM.2013.12.089.

[4] Gruwel MLH, Latta P, Matwiy B, Tomanek B. Characterization of food stuffs using Magnetic Resonance Elastography. Food Res Int 2010;43:2087–92. doi:10.1016/J.FOODRES.2010.07.015.

[5] Wu D, Sun D-W, He Y. Novel non-invasive distribution measurement of texture profile analysis (TPA) in salmon fillet by using visible and near infrared hyperspectral imaging. Food Chem 2014;145:417–26. doi:10.1016/j.foodchem.2013.08.063.

[6] Ma J, Sun D-W, Qu J-H, Liu D, Pu H, Gao W-H, et al. Applications of Computer Vision for Assessing Quality of Agri-food Products: A Review of Recent Research Advances. Crit Rev Food Sci Nutr 2016;56:113–27. doi:10.1080/10408398.2013.873885.

[7] Hussain A, Pu H, Sun D-W. Innovative nondestructive imaging techniques for ripening and maturity of fruits – A review of recent applications. Trends Food Sci Technol 2018;72:144–52. doi:10.1016/J.TIFS.2017.12.010.

[8] Basheer IA, Hajmeer M. Artificial neural networks: fundamentals, computing, design, and application. J Microbiol Methods 2000;43:3–31.

[9] Baiocco G, Tagliaferri V, Ucciardello N. Neural Networks Implementation for Analysis and Control of Heat Exchange Process in a Metal Foam Prototypal Device. In: DAddona D.M. TJ, editor. Procedia CIRP, vol. 62, Elsevier B.V.; 2017, p. 518–22. doi:10.1016/j.procir.2016.06.035.

[10] Baiocco G, Ucciardello N. Neural network implementation for the prediction of secondary phase precipitation and mechanical feature in a duplex stainless steel. Appl Phys A Mater Sci Process 2019;125:20. doi:10.1007/s00339-018-2312-z.

[11] Lorenz C, Ferraudo AS, Suesdek L. Artificial Neural Network applied as a methodology of mosquito species identification. Acta Trop 2015;152:165–9. doi:10.1016/J.ACTATROPICA.2015.09.011.

[12] Costanza G, Tata ME, Ucciardello N. Superplasticity in PbSn60: Experimental and neural network implementation. Comput Mater Sci 2006;37:226–33. doi:10.1016/j.commatsci.2005.06.009.

[13] Guarino S, Ucciardello N, Tagliaferri V. An application of neural network solutions to modeling of diode laser assisted forming process of AA6082 thin sheets. Key Eng Mater 2007;344:325–32. doi:10.4028/0-87849-437-5.325.

[14] Lucignano C, Montanari R, Tagliaferri V, Ucciardello N. Artificial neural networks to optimize the extrusion of an aluminium alloy. J Intell Manuf 2010;21:569–74. doi:10.1007/s10845-009-0239-0.

[15] Missori S, Sili A, Ucciardello N. Process parameters optimization of laser beam welded joints by neural network. Mater Manuf Process 2008;23:169–74. doi:10.1080/10426910701774692.

[16] Portalés C, Ribes-Gómez E. An image-based system to preliminary assess the quality of grape harvest batches on arrival at the winery. Comput Ind 2015;68:105–15. doi:10.1016/j.compind.2014.12.010.

[17] Walczak S, Velanovich V. Improving prognosis and reducing decision regret for pancreatic cancer treatment using artificial neural networks. Decis Support Syst 2018;106:110–8. doi:10.1016/j.dss.2017.12.007.

[18] Simoncini A, Tagliaferri V, Trovalusci F, Ucciardello N. Neural networks approach for IR-heating and deformation of ABS in thermoforming. Int J Comput Appl Technol 2017;56:114. doi:10.1504/IJCAT.2017.087333.

[19] Donnini R, Montanari R, Santo L, Tagliaferri V, Ucciardello N. Implementation of neural network for the thrust force prediction in hot drilling of 6082 aluminium alloy. Int J Comput Mater Sci Surf Eng 2010;3:175. doi:10.1504/IJCMSSE.2010.033152.

[20] Costanza G, Tata ME, Ucciardello N. Application of neural network to the materials characterisation. Int J Comput Mater Sci Surf Eng 2010;3:96–113. doi:10.1504/IJCMSSE.2010.033147.

[21] Lashkia V. Defect detection in X-ray images using fuzzy reasoning. Image Vis Comput 2001;19:261–9. doi:10.1016/S0262-8856(00)00075-5.

[22] Valavanis I, Kosmopoulos D. Multiclass defect detection and classification in weld radiographic images using geometric and texture features. Expert Syst Appl 2010;37:7606–14. doi:10.1016/J.ESWA.2010.04.082.

[23] Sabzi S, Arribas JI. A visible-range computer-vision system for automated, non-intrusive assessment of the pH value in Thomson oranges. Comput Ind 2018;99:69–82. doi:10.1016/J.COMPIND.2018.03.016.

[24] Jahedsaravani A, Massinaei M, Marhaban MH. Application of Image Processing and Adaptive Neuro-fuzzy System for Estimation of the Metallurgical Parameters of a Flotation Process. Chem Eng Commun 2016;203:1395–402. doi:10.1080/00986445.2016.1198897.

[25] Costa YMG, Oliveira LS, Koerich AL, Gouyon F, Martins JG. Music genre classification using LBP textural features. Signal Processing 2012;92:2723–37. doi:10.1016/J.SIGPRO.2012.04.023.

[26] Philip J, Bharadi VA. Signature Verification SaaS Implementation on Microsoft Azure Cloud. Procedia Comput Sci 2016;79:410–8. doi:10.1016/J.PROCS.2016.03.053.

[27] LeCun Y, Boser B, Denker JS, Henderson D, Howard RE, Hubbard W, et al. Backpropagation Applied to Handwritten Zip Code Recognition. Neural Comput 1989;1:541–51. doi:10.1162/neco.1989.1.4.541.

[28] Krizhevsky A, Sutskever I, Hinton GE. ImageNet classification with deep convolutional neural networks. Commun ACM 2017;60:84–90. doi:10.1145/3065386.

[29] Niu X-X, Suen CY. A novel hybrid CNN–SVM classifier for recognizing handwritten digits. Pattern Recognit 2012;45:1318–25. doi:10.1016/J.PATCOG.2011.09.021.

[30] Boaretto N, Centeno TM. Automated detection of welding defects in pipelines from radiographic images DWDI. NDT E Int 2017;86:7–13. doi:10.1016/J.NDTEINT.2016.11.003.

[31] Costa YMG, Oliveira LS, Silla CN. An evaluation of Convolutional Neural Networks for music classification using spectrograms. Appl Soft Comput 2017;52:28–38. doi:10.1016/J.ASOC.2016.12.024.

[32] Blasco J, Aleixos N, Gómez J, Moltó E. Citrus sorting by identification of the most common defects using multispectral computer vision. J Food Eng 2007;83:384–93. doi:10.1016/J.JFOODENG.2007.03.027.

[33] Kılıç K, Boyacı İH, Köksel H, Küsmenoğlu İ. A classification system for beans using computer vision system and artificial neural networks. J Food Eng 2007;78:897–904. doi:10.1016/J.JFOODENG.2005.11.030.

[34] Zhang Y, Wang S, Ji G, Phillips P. Fruit classification using computer vision and feedforward neural network. J Food Eng 2014;143:167–77. doi:10.1016/J.JFOODENG.2014.07.001.

[35] Li J, Rao X, Ying Y. Detection of common defects on oranges using hyperspectral reflectance imaging. Comput Electron Agric 2011;78:38–48. doi:10.1016/J.COMPAG.2011.05.010.

[36] Li Q, Wang M, Gu W. Computer vision based system for apple surface defect detection. Comput Electron Agric 2002;36:215–23. doi:10.1016/S0168-1699(02)00093-5.

[37] Sabzi S, Abbaspour-Gilandeh Y, García-Mateos G. A fast and accurate expert system for weed identification in potato crops using metaheuristic algorithms. Comput Ind 2018;98:80–9. doi:10.1016/J.COMPIND.2018.03.001.

[38] Almonti D, Ucciardello N. Design and Thermal Comparison of Random Structures Realized by Indirect Additive Manufacturing. Mater (Basel, Switzerland) 2019;12. doi:10.3390/ma12142261.

[39] Almonti D, Ucciardello N. Improvement of thermal properties of micro head engine electroplated by graphene: experimental and thermal simulation. Mater Manuf Process 2019:1–8. doi:10.1080/10426914.2019.1594263.

[40] Almonti D, Simoncini M, Tagliaferri V, Ucciardello N. Electro-deposition of graphene nanoplatelets on CPU cooler—experimental and numerical investigation. Mater Manuf Process 2018;33:220–6. doi:10.1080/10426914.2017.1303165.

[41] Guarino S, Ponticelli GS. High Power Diode Laser (HPDL) for Fatigue Life Improvement of Steel: Numerical Modelling. Metals (Basel) 2017;7:447. doi:10.3390/met7100447.

[42] Ponticelli GS, Guarino S, Giannini O. A fuzzy logic-based model in laser-assisted bending springback control. Int J Adv Manuf Technol 2018;95:3887–98. doi:10.1007/s00170-017-1482-8.

[43] Ponticelli GS, Guarino S, Tagliaferri V, Giannini O. An optimized fuzzy-genetic algorithm for metal foam manufacturing process control. Int J Adv Manuf Technol 2019;101:603–14. doi:10.1007/s00170-018-2942-5.